Characterizing eigenstate thermalization via measures in the Fock space of operators

Pavan Hosur and Xiao-Liang Qi

Characterizing eigenstate thermalization via measures in the Fock space of operators

Pavan Hosur and Xiao-Liang Qi

Department of Physics, Stanford University, Stanford, CA 94305-4045, USA

The eigenstate thermalization hypothesis (ETH) attempts to bridge the gap between quantum mechanical and statistical mechanical descriptions of isolated quantum systems. Here, we define unbiased measures for how well the ETH works in various regimes, by mapping general interacting quantum systems on regular lattices onto a single particle living on a high-dimensional graph. By numerically analyzing deviations from ETH behavior in the non-integrable Ising model, we propose a quantity that we call the *n-weight* to democratically characterize the average deviations for all operators residing on a given number of sites, irrespective of their spatial structure. It appears to have a simple scaling form, that we conjecture to hold true for all non-integrable systems. A closely related quantity, that we term the *n-distinguishability*, tells us how well two states can be distinguished if only *n*-site operators are measured. Along the way, we discover that complicated operators on average are worse than simple ones at distinguishing between neighboring eigenstates, contrary to the naive intuition created by the usual statements of the ETH that few-body (many-body) operators acquire the same (different) expectation values in nearby eigenstates at finite energy density. Finally, we sketch heuristic arguments that the ETH originates from the limited ability of simple operators to distinguish between quantum states of a system, especially when the states are subject to constraints such as roughly fixed energy with respect to a local Hamiltonian.

I. INTRODUCTION

Statistical mechanics and quantum mechanics have been the cornerstones of modern physics for nearly a century. Both formalisms have been put to test in a wide variety of scenarios, and both have invariably given descriptions that are accurate as well as consistent with each other within their regimes of validity. Their starting points, however, are fundamentally different. Quantum mechanics describes unitary evolution of isolated systems via wave functions or pure states, whereas statistical mechanics ascribes microcanonical ensembles – which are inherently mixed states – to them. Why, then, do the two theories concur?

A crucial step towards answering this question was taken by Berry [1], who conjectured that the eigenstates of quantum Hamiltonians whose classical counterparts are chaotic behave as if they were drawn randomly from a Gaussian distribution. In other words, they resemble random superpositions of classical configurations at the same energy density in the thermodynamic limit. Deutsch [2] argued that Berry's conjecture holds for integrable systems perturbed away from integrability. The argument stems from the intuition that integrability-breaking perturbations allow quantum systems to mimic the central maxim of classical statistical mechanics. On the one hand, classical ergodic systems explore all accessible microstates with equal likelihood within the time scale of typical measurements and hence, justify equating time and ensemble averages. On the other, quantum systems can access all classical "microstates" *at once* from a single eigenstate, so no time or ensemble-averaging is required and each eigenstate effectively resembles a microcanonical ensemble. Srednicki [3] then explicitly derived statistical distributions for quantum particles assuming only Berry's conjecture, and postulated the *eigenstate thermalization hypothesis* (ETH).

The *weak* form of the ETH addresses long time behavior of states after a quantum quench to a non-integrable Hamiltonian, and says that they resemble thermal ensembles, with exponentially small corrections in the system size, at most times with respect to the measurement of "simple" observables. Here, "simple" operators usually refers to operators that involve a very small number of degrees of freedom compared to the system size, although the precise definition is given very rarely [4]. This requires diagonal matrix elements of these operators in the energy eigenstate basis to vary smoothly with energy, with exponentially small fluctuations, and off-diagonal elements to be exponentially small. The *strong* form, on the other hand, states that individual finite energy density eigenstates of non-integrable Hamiltonians resemble thermal ensembles if only simple observables are measured, and actually implies the condition on the diagonal matrix elements that was required for the weak form. In this work, we focus only on this condition. In other words, after precisely defining what we mean by "simple", we will investigate how different the expectation values of operators in eigenstates neighboring in energy are, as a function of how "simple" or "complicated" the operator is. Off-diagonal matrix elements, as well as the differences between eigenstates and thermal ensembles, will be analyzed in future work.

The ETH is only believed to hold for simple operators and states with finite energy density in the thermodynamic limit. With increasing complexity of operators, their ability to tell eigenstates with nearby energy apart improves. The extreme case is that of a projection operator $\rho_n = |n\rangle\langle n|$ onto a given eigenstate $|n\rangle$; this typically has support on all sites of the system and it obviously distinguishes $|n\rangle$ from all other eigenstates perfectly. Therefore, a refined statement of the ETH demands the definition of quantitative measures for how distinguishable two states are when a restricted set of operators is measured.

Moreover, we will see that choosing this restricted set to be all operators of certain complexity (rather than some arbitrarily chosen operators) permits the definition of a "basis-independent measure" to systematically quantify how well the ETH works and how distinguishable nearby states are as a function of the system size, eigenstate energy and operator complexity.

In this work, we define two such measures:

1. the n-weight of a Hermitian operator A,

$$P_n(A) = \sum_\ell \left| \text{Tr}\left(A O_\ell^{(n)} \right) \right|^2 \qquad (1)$$

where $O_\ell^{(n)}$ for all ℓ form a complete orthonormal basis (with respect to the Hilbert-Schmidt norm) of operators that have support on n sites, and

2. the n-distinguishability of two operators A_1 and A_2,

$$\theta_n(A_1, A_2) = \cos^{-1} \frac{P_n(A_1) + P_n(A_2) - P_n(A_1 - A_2)}{2\sqrt{P_n(A_1)P_n(A_2)}} \qquad (2)$$

Geometrically, $P_n(A)$ is the squared norm of the projection of A onto the space of n-site operators, while $\theta_n(A_1, A_2)$ is the angle between the projections of A_1 and A_2. These measures are defined for a lattice system with the Hilbert space $\mathbb{H} = \prod_i^\otimes \mathbb{H}_i$, $\mathbb{H}_i$ being the Hilbert space of the ith site. The intuition behind these quantities is an alternative view of quantum many-body dynamics. As will be described in Sec. II, Heisenberg evolution of a many-body operator can be mapped to a quantum mechanical problem of a single particle hopping on a high-dimensional graph. Each site of the graph represents a basis operator, e.g., a direct product of Pauli operators if each lattice site hosts a single qubit. The "particle wavefunction" is determined by the overlap of operator A with the basis operator. The graph has a layered structure with all n-site operators $O_\ell^{(n)}$ in the n-th layer. In this picture, the n-weight $P_n(A)$ is simply proportional to the probability of the particle being in the n-th layer of the graph. The n-distinguishability of two operators A_1 and A_2 is the angle between the projections of the corresponding vectors in the Hilbert space of operators onto the subspace of the graph sites that constitute the nth layer. A large angle θ_n means A_1 and A_2 are easier to distinguish with n-site operators.

Most previous studies have numerically analyzed the expectation values or off-diagonal matrix elements of a select set of simple operators dwelling in contiguous regions of space either at long times [5–11] or in different eigenstates [12–18]. Infinite temperature studies are the only exceptions that we are aware of that include non-contiguous regions of space [19–23]. In contrast, our measures treat all operators with support on a given number of sites on equal footing, irrespective of whether the sites are adjacent or spatially separated. Thus, they are unbiased with respect to the choice of operators of a given

size, as well as to the on-site basis in real space used to represent them. Moreover, we will see shortly in Sec III that they possess neat mathematical properties that make their computation relatively easy. They are also related to some simple physical quantities. In particular, if A is chosen to be a density operator, then the n-weight turns out to be closely related to the second Renyi entropy of regions with size n and smaller. However, the Renyi entropy of an n-site region has contributions from fewer site operators too, while the n-weight is a direct measure of the amplitude of n-site correlation functions in this density operator.

Using the two measures we define, we study two related quantities that characterize the difference between two neighboring eigenstates, with density operators ρ_1 and ρ_2. The first quantity is the n-weight of the difference, $P_n(\rho_1 - \rho_2)$. By performing numerical exact diagonalization on a simple non-integrable model, an Ising model with parallel and transverse fields, we discover that $P_n(\rho_1 - \rho_2)$ attains a simple scaling form as a function of n and the density of states in the part of the spectrum from which the two states are drawn. We conjecture that a similar form holds in all non-integrable systems. Our result on $P_n(\rho_1 - \rho_2)$ also clarifies a rather peculiar feature of quantum ergodic systems. According to the ETH, one would naively think that a complicated (high n) operator has a better chance of distinguishing two neighboring eigenstates than a simple operator. We discover that surprisingly, the opposite is true for typical operators: simple operators *on average* are better at distinguishing between nearby eigenstates than complicated operators are. In fact, there is a critical size of operators, which only depends on the system size and the Hilbert space dimension at each site, at which measuring a random operator reveals no information about the system. This critical operator size occurs well beyond half of the system size, and was consequently missed by previous studies that focused on simple operators.

The second quantity we study is the n-distinguishability for the same pair of eigenstates, $\theta_n(\rho_1, \rho_2)$, which helps to reconcile the intuition and the numerical observation mentioned above. This angle is found to be small when the vectors are projected onto a low-n subspace, determined by simple operators, but to saturate to $\pi/2$ for more complex operators. Both these behaviors are found to be strikingly different in integrable systems. The large n-distinguishability suggests that although most large operators are poor at distinguishing between neighboring eigenstates, there are a few fine-tuned ones that are proficient at it. Thus, the optimal n-site operator can differentiate between the two states better if n is large, but a randomly chosen one works better for smaller n. The combination of the two measures P_n and θ_n thus provides a more systematic and accurate understanding of the nature of thermalization.

The remainder of the paper is organized as following. In Sec. II we describe the Fock space of operators and set the general framework of our approach. The two quan-

tities n-weight and n-distinguishability are defined and their general properties are discussed in Sec. III. Sec. IV is devoted to analyzing numerical results in the Ising model, while Sec. V is dedicated to further discussions and conclusion.

II. FOCK SPACE OF OPERATORS

We start by defining a mapping from a lattice many-body system to a single-particle quantum mechanics problem on a high-dimensional graph. For concreteness and simplicity, let us choose the many body system to be a spin-1/2 model with Hamiltonian H on a chain with L sites. For a spin-1/2 model, the Hilbert space of site r is spanned by an orthonormal basis consisting of the identity matrix and the Pauli matrices: $\frac{1}{\sqrt{2}} \left(\mathbb{1}_r, \sigma_r^x, \sigma_r^y, \sigma_r^z \right) \equiv O_{(r,i)}, i = 0, 1, 2, 3$, normalized as $\mathrm{Tr}\left(O_{(r,i)} O_{(r,j)} \right) = \delta_{ij}$. They satisfy the orthogonality condition

$$\sum_{i=1}^{3} O_{(r,i)}^{ab} O_{(r,i)}^{cd} = \delta_{ad}\delta_{bc} - \frac{1}{D}\delta_{ab}\delta_{cd} \equiv W_r = X_r - \frac{\mathbb{1}_r}{D} \quad (3)$$

where $D = 2$ is the dimension of the Hilbert space at each site, $X_r^{ab,cd} = \delta_{ad}\delta_{bc}$ is the "swap" operator acting on site r, whose expectation value computed over two copies of any state ρ is related to the second Renyi entropy of site r in that state [24]: $S_r = -\log \mathrm{Tr}_{\bar{r}} \left(\mathrm{Tr}_r \rho \right)^2 = -\log \mathrm{Tr} \left[(\rho \otimes \rho) X_r \right]$, and W_r is its traceless part. Here, $\bar{r}$ denotes all sites except site r. The Hilbert space of the whole system is spanned by multisite operators $O_{\{r_\alpha, i_\alpha | \alpha = 1...n\}}^{(n)} = O_{(r_1,i_1)} \otimes O_{(r_2,i_2)} \ldots O_{(r_n,i_n)} \equiv O_\ell^{(n)}$, where n represents the number of sites on which $O_\ell^{(n)}$ is one of the Pauli matrices, and sites absent in the set $\{r_\alpha\}$ are assumed to host the normalized identity operator $\frac{\mathbb{1}}{\sqrt{2}}$ in $O_\ell^{(n)}$. Henceforth, n will be referred to as the *size* of the operator $O_\ell^{(n)}$. The subscript ℓ indexes all operators with size n, so it runs from 1 through $(D^2 - 1)^n \binom{L}{n} \equiv f_n D^{2L}$. We will refer to operators with small (large) n as simple (complicated) operators.

Now, we construct a graph by assigning a node to each basis operator $O_\ell^{(n)}$. The nodes are sorted by operator-size, so the nth layer of the graph is comprised of nodes corresponding to n-site operators, as depicted in Fig. 1. The total number of operators, or nodes in the graph, is D^{2L}, while the number of nodes in each layer is $f_n D^{2L}$. The outline in Fig. 1 depicts the number of nodes in each layer, $f_n D^{2L}$. For $L \gg D^2$, f_n is maximized at $n = n^* = (1 - 1/D^2)L$ which equals $3L/4$ for $D = 2$. It is easy to check that n^* is the mean, median as well as the mode of f_n. Physically, this means that a randomly chosen basis operator is most likely to have a size of n^*, since each site has $D^2 - 1$ non-trivial operators and a single trivial one.
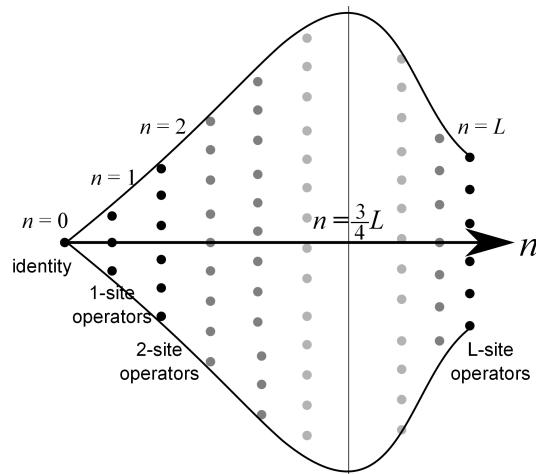

Figure 1. Schematic of the tree network, constructed by arranging operators according to their size. The identity operator is on the extreme left, followed by the single-site operators, and so on. The total number of operators is D^{2L}, while the fraction in the nth layer is $f_n = \frac{(D^2-1)^n}{D^{2L}} \binom{L}{n}$, which is maximum for $n = (1 - 1/D^2)L = \frac{3}{4}L \equiv n^*$ for $D = 2$. Note that f_n grows exponentially with n for small n, so the apparent linear growth in the number of dots with n in the figure is for ease of depiction and should not be taken literally.

The orthogonality of the operator basis allows us to expand an arbitrary many-body Hermitian operator $A(t)$ in this basis as $A(t) = \sum_{n,\ell} \psi_{n\ell}(A;t) O_\ell^{(n)}$, with real coefficients:

$$\psi_{n\ell}(A;t) = \mathrm{Tr}\left(A(t) O_\ell^{(n)} \right) \quad (4)$$

The vector $\psi_{n\ell}(A;t)$ can be viewed as a "single-particle wavefunction" of a particle hopping on the graph we defined. There are two key requirements for interpreting $\psi_{n\ell}(A;t)$ as a sensible single-particle wavefunction within first quantization. Firstly, the total probability density of the particle must be conserved; this is guaranteed because $\left\{ O_\ell^{(n)} \right\}$ form an orthonormal basis for operators in the Hilbert space, which implies

$$\sum_{n,\ell} |\psi_{n\ell}(A;t)|^2 = \mathrm{Tr}\left(A^2 \right) \quad (5)$$

a manifestly invariant quantity under unitary time-evolution of A. Secondly, it must satisfy Schrodinger's equation. Indeed, $A(t)$ follows Heisenberg time evolution: $\dot{A}(t) = i[H, A(t)]$, so the time-evolution of $\psi_{n\ell}$ is given by

$$i\frac{\partial}{\partial t}\psi_{n\ell}(A;t) = \mathrm{Tr}\left([A(t), H] O_\ell^{(n)} \right)$$
$$= \mathcal{H}_{\ell\ell'}^{nn'} \psi_{n'\ell'}(A;t) \quad (6)$$

where the hopping matrix element between two nodes $O_\ell^{(n)}$ and $O_{\ell'}^{(n')}$ is defined as

$$\mathcal{H}_{\ell\ell'}^{nn'} = \text{Tr}\left(\left[H, O_\ell^{(n)}\right] O_{\ell'}^{(n')}\right) = -\mathcal{H}_{\ell'\ell}^{n'n} = -\left(\mathcal{H}_{\ell\ell'}^{nn'}\right)^* \tag{7}$$

Thus, $\psi_{n\ell}(A;t)$ is a sensible wavefunction, and its dynamics are governed by the hopping Hamiltonian (7). Crucially, if the physical Hamiltonian contains at most k-spin terms, $\mathcal{H}_{\ell\ell'}^{nn'}$ vanishes for $|n - n'| \geq k$ and therefore, satisfies a notion of locality on the graph. Thus, the time-evolution of a general operator in a many body system has been recast into the problem of a single particle governed by a local hopping Hamiltonian on a high-dimensional graph. The "energies" of the particle consists of all possible differences $E_i - E_j; i, j = 1 \ldots D^L$ between pairs of energies of H, so the single-particle spectrum that results from a generic H with no degeneracies is particle-hole symmetric with D^L zero eigenvalues and $D^{2L} - D^L$ non-zero ones. The above construction is reminiscent of mappings of states in Fock space to a Cayley tree, which allows one to view integrable systems with local conservation laws in real [25] and momentum [26] space as a localized particle on a suitably defined tree. Our construction, on the other hand, describes the Fock space of operators instead of that of states, and thus is closer to the approach adopted by Ref. [27] for constructing integrals of motion to the describe the many-body localized phase.

The graph construction facilitates extracting different kinds of information about quantum ergodicity with different choices of A. If we choose A to be the density matrix ρ for an eigenstate that satisfies the ETH, then $\psi_{n\ell}(A)$ is expected to coincide with its thermal value, determined only by the energy density in that state, for small n, but can be depend on other details for larger n. On the other hand, picking A to be the difference between two density matrices tells us how various correlators differ in the two states, and what kind of observables must be measured in order to distinguish between them. Finally, if A is a physical observable O, its time-evolution tells us how this physical quantity evolves into a superposition of other operators with time. In particular, suppose we start from a small-n operator and let it evolve in time. In general, it will evolve into a superposition containing many large-n operators. Equivalently, one can think of $\psi_{n\ell}(O;t)$ as an infinite temperature correlation function, so its time evolution tells us how small operators develop correlations with large operators over time. In the language of the hopping particle, this corresponds to the particle starting near the low-n end of the graph and spreading towards larger n nodes. Thus, chaotic behavior of operators turns into delocalization of the particle on the graph.

III. n-WEIGHT AND n-DISTINGUISHABILITY

A central quantity that we will work with in this paper is the n-weight of an operator A, $P_n(A)$, defined as

$$P_n(A) = \sum_\ell |\psi_{n\ell}(A)|^2 = \sum_{\{r_\alpha, i_\alpha\}} \left|\text{Tr}\left(AO_{\{r_\alpha, i_\alpha|\alpha=1\ldots n\}}\right)\right|^2 \tag{8}$$

where the sum over ℓ runs over all possible choices of n-site operators. As mentioned earlier, $P_n(A)$ is the norm squared of the vector $\vec{\psi}_n(A) = \psi_{n\ell}(A) = \text{Tr}\left(AO_\ell^{(n)}\right)$. In the graph picture of Sec. II, this is the total probability density in the nth layer of the graph. Physically, $P_n(A)$ tells us how complex the correlators one must measure in order to reconstruct A are. Computing it directly is computationally taxing, as it entails computing D^{2L} traces, one for each operator in the Hilbert space. Fortunately, the computation can be simplified via a generating function, as follows.

Performing the sums over $\{i_\alpha\}$ for fixed $\{r_\alpha\}$ and using Eq. (3) gives

$$P_n(A) = \frac{1}{D^{L-n}} \sum_{R_n} \prod_{r \in R_n} \text{Tr}\left[(A \otimes A)W_r\right] \tag{9}$$

where R_n is a region of size n (not necessarily connected), and the sum $\sum_{R_n}$ is over all n-site regions. Now we define a generating function

$$F(A; z) = \sum_{n=0}^{L} z^n P_n(A) \tag{10}$$

which can be explicitly written as

$$F(A; z) = \frac{1}{D^L} \text{Tr}\left[A \otimes A \prod_{r=1}^{L}\left(\mathbb{1}_r + Dz W_r\right)\right] \tag{11}$$

$$= \frac{1}{D^L} \sum_R (1-z)^{L-k_R}(Dz)^{k_R} \text{Tr}_R\left(\text{Tr}_{\bar{R}} A\right)^2$$

Here the sum $\sum_R$ is over all regions R, composed of k_R sites and $\bar{R}$ denotes the complement of R. $P_n(A)$ is then determined by Fourier transforming $F(A; e^{in\theta})$:

$$P_n(A) = \frac{1}{2\pi} \int d\theta e^{-in\theta} F(A; e^{in\theta}) \tag{12}$$

Since $n \in [0, L]$ is linear in system size, it is actually sufficient to calculate $F(A; e^{in\theta})$ for the $L+1$ discrete values of $\theta = \frac{2\pi}{L+1}m, \ m = 0, 1, .., L$. Therefore we have translated the calculation of $P_n(A)$ for all A to $L+1$ operator trace computations in the doubled Hilbert space. Alternatively, we can also use the second line of Eq. (11) and calculate P_n by performing D^L partial trace calculations on a single copy of the system.

When A is a density matrix ρ, the generating function also makes it transparent that $P_n(A)$ is related to the second Renyi entropy of a region R, $S_R = -\log \text{Tr}(\rho_R)^2 =$

$-\log \text{Tr}\left[\rho \otimes \rho \prod_{r \in R} X_r\right]$. From (9), we have

$$P_n(\rho) = \frac{1}{D^{L-n}} \sum_{R_n} \sum_{R_k \subseteq R_n} e^{-S_{R_k}} \left(-\frac{1}{D}\right)^{n-k} \quad (13)$$

The sum over R_n and R_k can be combined into a single sum by introducing suitable combinatorial factors. Defining $e^{-\mathbb{S}_k} = \left\langle e^{-S_{R_k}} \right\rangle_{R_k}$, i.e., the average of $e^{-S_{R_k}}$ over all k-site regions, we get

$$P_n(\rho) = \frac{1}{D^{L-n}} \binom{L}{n} \sum_{k=0}^{n} e^{-\mathbb{S}_k} \left(-\frac{1}{D}\right)^{n-k} \binom{n}{k} \quad (14)$$

Thus, there is a simple relationship between P_n, the "single particle density on the graph", and entanglement properties of the many body state.

Based on the n-weight defined for each operator A, we define a second quantity, the n-distinguishability between two operators A_1 and A_2, as the angle between the two vectors $\vec{\psi}_n(A_1)$ and $\vec{\psi}_n(A_2)$:

$$\theta_n(A_1, A_2) = \cos^{-1} \frac{\vec{\psi}_n(A_1) \cdot \vec{\psi}_n(A_2)}{|\vec{\psi}_n(A_1)||\vec{\psi}_n(A_2)|} \quad (15)$$

angle between the Hilbert space vectors for the two "single particle wavefunctions" corresponding to A_1 and A_2, projected to the graph sites corresponding to size-n operators. This definition is identical to (2) stated earlier. The angle θ_n thus measures how different the two operators are if only overlaps with n-site operators are measured. A small θ_n implies that A_1 and A_2 look similar in all size-n measurements, while a large $\theta_n \sim \frac{\pi}{2}$ means A_1 and A_2 can be easily distinguished by n-site operators. This is sketched in Fig. 2, where we have chosen $A_{1,2}$ to be two density matrices $\rho_{1,2}$ in anticipation of the discussion in the next section. In Sec. IV B, we will use θ_n to distinguish between neighboring eigenstates and show that indeed, they appear similar for simple observables and different for complicated ones.

IV. EIGENSTATE THERMALIZATION IN THE ISING MODEL

In this section we apply the new measures we define to study eigenstate thermalization in a prototypical non-integrable spin model, namely, the 1D Ising model with transverse and longitudinal fields, given by

$$H = \sum_r \left(J\sigma_r^z \sigma_{r+1}^z + h_x \sigma_r^x + h_z \sigma_r^z \right) + h_z \sigma_1^z \quad (16)$$

H is integrable if any one of J, h_x and h_z vanishes, but is non-integrable otherwise. We choose $J = 0.5$, $h_x = -0.74$ and $h_z = 0.35$ as the non-integrable parameters, and $J = 0.5$, $h_x = 0.35$ and $h_z = 0$ as the integrable ones. Open boundary conditions and the extra term on
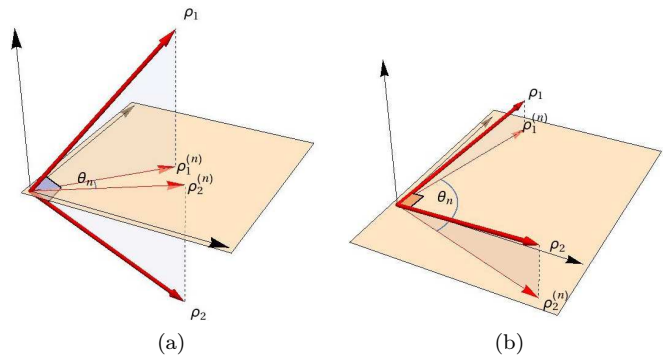

Figure 2. Schematic illustration of the behavior of neighboring eigenstates ρ_1 and ρ_2 on being projected onto the space of small-n (a) and large-n (b) operators. $\rho_i^{(n)}$ is shorthand for the projections $\vec{\psi}_n(\rho_i)$ defined in the text. The three directions together depict the full Hilbert space of operators, while the horizontal plane represents its projection onto the space of operators of size n. ρ_1 and ρ_2 are mutually orthogonal vectors in the full space. However, they appear nearly identical when projected onto simple operators as shown on the left, but look quite different for larger operators as shown on the right. The angle θ_n will be calculated numerically for the non-integrable Ising model in Sec. IV.
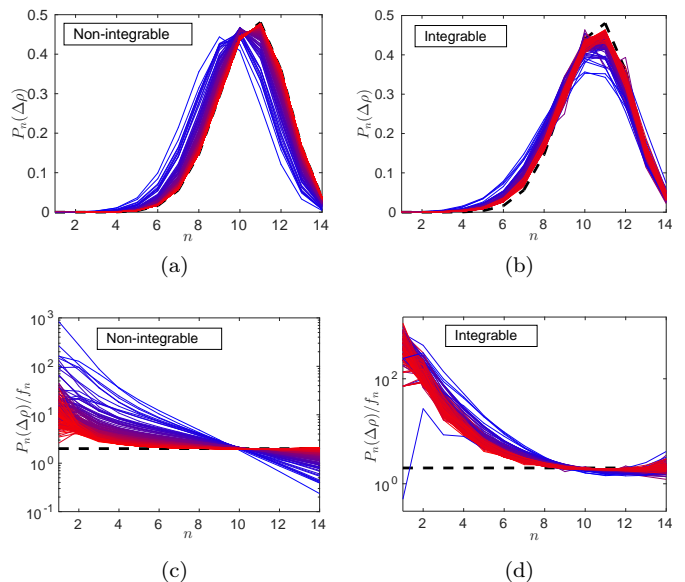

Figure 3. $P_n(\Delta\rho)$ vs n (a,b) and $P_n(\Delta\rho)/f_n$ vs n (c,d) for ~ 200 randomly chosen pairs of neighboring eigenstates for $L = 14$ sites for the ergodic (a,c) and the integrable (b,d) Ising model. Here, $\Delta\rho = \rho_1 - \rho_2$ is the difference between the density matrices of the two eigenstates. The color is proportional to the density of states, with blue (red) representing states in regions of the spectrum with low (high) density of states. The black dashed line marks $P_n(\Delta\rho) = 2f_n$.

the first site, $h_z\sigma_1^z$, ensure that translation and inversion symmetries are broken so that there are no conserved quantities in the non-integrable case. This is unlike several recent works which retained translational symmetry and hence, conserved the total momentum [4, 6, 12, 28]. The energies and eigenstates are obtained by exact diagonalization of systems of upto $L = 14$ sites.

A. Comparison of eigenstate n-weights

As stated in the introduction, the ETH says that the expectation values of simple operators are equal in nearby eigenstates of chaotic Hamiltonians, up to exponentially small corrections in the system size. This automatically ensures that each eigenstate resembles a "microcanonical ensemble", i.e., an equal admixture of nearby eigenstates, in the thermodynamic limit and hence yields the ETH as stated in the introduction. Thus, we first compare pairs of neighboring eigenstates ρ_1 and ρ_2 by computing the total squared difference in the expectation values of all operators of size n,

$$P_n(\Delta\rho) = \sum_\ell \left(\left\langle O_\ell^{(n)} \right\rangle_{\rho_1} - \left\langle O_\ell^{(n)} \right\rangle_{\rho_2} \right)^2 \qquad (17)$$

where $\Delta\rho = \rho_1 - \rho_2$, and study its dependence on n and the energy of the pair. As shown in the upper panels of Fig. 3, this quantity has the anticipated behavior for small n: it increases with n and is larger when the density of states is lower. A closer inspection, however, reveals that the n-dependence seen here is deceptive, and cannot be used to declare eigenstate thermalization. In particular, the curves approximately follow the fraction of operators of size n, $f_n = \frac{(D^2-1)^n}{D^{2L}} \binom{L}{n}$ upto an overall proportionality constant. In fact, the "infinite temperature" eigenstates – states near the middle of the spectrum where the density of states is highest – have $P_n(\Delta\rho) \approx 2f_n = \mathrm{Tr}\left[(\Delta\rho)^2\right] f_n$. Moreover, the n-dependence is roughly the same even for the integrable Ising model. Thus, we conclude that the bare n-dependence of $P_n(\Delta\rho)$ is primarily determined by the number of operators of size n, not by the integrability properties of the Hamiltonian.

Therefore we study the average density per site $P_n(\Delta\rho)/f_n$ – the mean squared difference in the expectation values of size-n operators between neighboring eigenstates, upto an overall proportionality constant of D^{2L}. As is shown in the lower panels of Fig. 3, the n-dependence of this quantity is clearly different for ergodic and integrable systems. However, its n-dependence for the ergodic system is the exact opposite of what one would naively expect from ETH. Indeed, the lower panels of Fig. 3 show that on average, large operators are actually worse at distinguishing between neighboring eigenstates than small operators are, irrespective of whether the Hamiltonian is integrable or not.

The fact that $P_n(\Delta\rho)/f_n$ decreases with n for small n simply says that on average, simple operators store more information about the state of the system compared to complicated ones. For integrable systems as well as for ground states of ergodic systems, this statement is easily understood because nearby eigenstates *can* be distinguished by simple operators. Fig. 3 says that random simple operators can split finite energy density states of ergodic Hamiltonians as well, but the efficiency with which they can do so decreases with increasing density of states. For the infinite temperature states (i.e., states at the part of the spectrum with the largest density of states) P_n/f_n is almost independent of n, which means that there is no difference between simple and complicated operators, since the state is essentially a random state in the Hilbert space.

A peculiar feature of Fig. 3 is that random operators of size $n = n^* \approx 3L/4 = (1 - 1/D^2)L$ cannot distinguish between any pair of states, irrespective of the Hamiltonian. This can be understood heuristically as follows. Since each site has $D^2 - 1$ non-trivial operator and a single trivial operator, a random operator has size n^*. The concurrence of $P_n(\Delta\rho)/f_n$ curves at $n = n^*$ reflects the fact that measuring a random operator does not reveal any information about the state of the system. Random operators with $n > n^*$ can again distinguish between neighboring eigenstates. Unlike simple operators, however, the efficiency with which they can do so in ergodic systems increases with increasing density of states. In other words, random operators with $n < n^*$ are better at splitting low lying excitations than at splitting finite energy density states, whereas operators with $n > n^*$ are better at the opposite.

Although P_n/f_n decreases with n for both ergodic and integrable systems, its dependence on the density of states is clearly different, as can be seen from Fig. 3. Thus, we highlight the difference by plotting the same data as a function of the density of states $g(E)$ in Fig. 4. Interestingly, for the non-integrable model we find that both the n-dependence and the density-of-states dependence can be captured by a clear scaling form given by

$$\frac{P_n(\Delta\rho)}{f_n} \approx \left(\frac{g(E)}{g_\infty} \right)^{a(n/n^*-1)} \mathcal{S}\left(\frac{n}{L} \right) \qquad (18)$$

where $g_\infty = \max g(E)$, a is a positive constant and $\mathcal{S}(n/L)$ is a scaling function of $O(1)$ that depends only weakly on n/L; for the data shown in this section it is the exponential of a simple polynomial (See Fig. 4, right bottom). Eq. (18) depends mainly on generic properties of the system such as the density of states of the spectrum, the Hilbert space dimension on each site and the system size. These properties are obviously common to both integrable and ergodic systems; in fact, the scaling of $g(E)$ with system size shows no distinction between them, as one can see in the left panel of Fig. 4, and $P_n(\Delta\rho)/f_n$ seems to be roughly energy-independent. However, we see that integrable systems do not have simple scaling
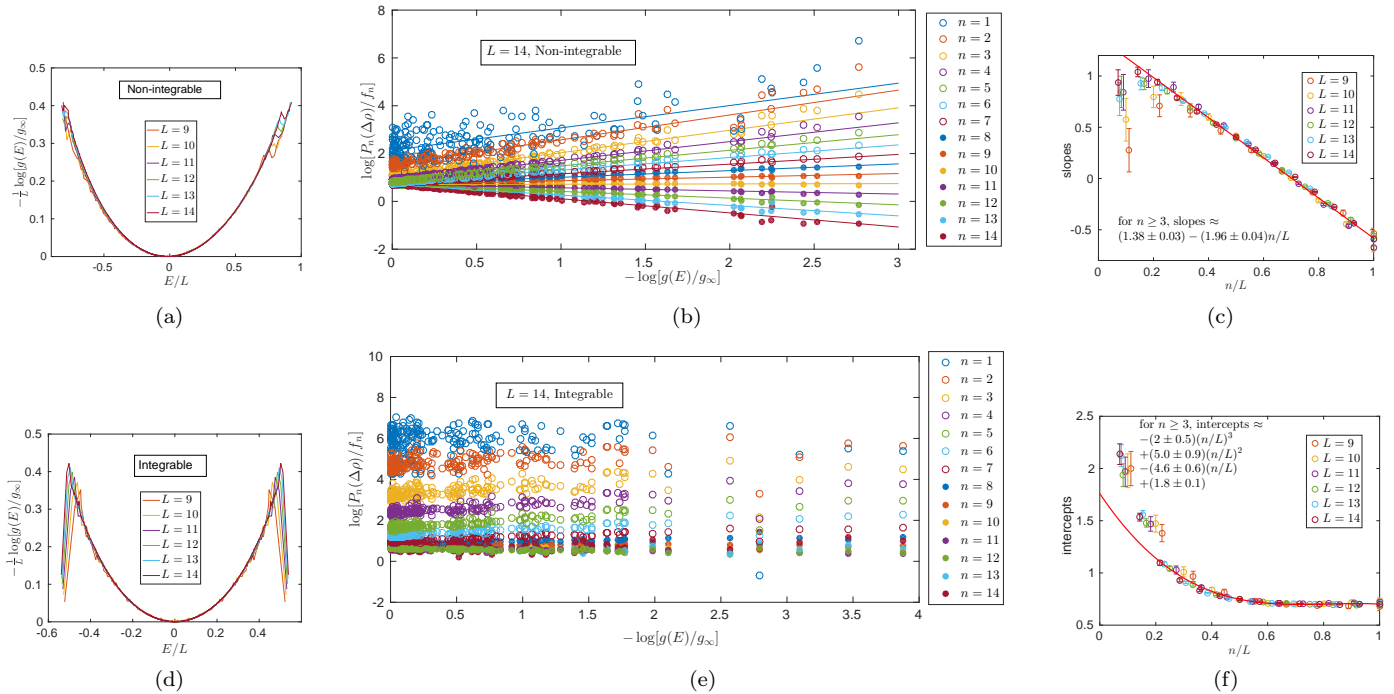
Figure 4. Left: $\frac{1}{L}\log\left[g_\infty/g(E)\right]$ vs the energy density E/L for various system sizes for the non-integrable (a) and the integrable (d) Ising model. Except near the band edges, the curves are indistinguishable, indicating that $g(E)/g_\infty$ grows exponentially with L with an energy density dependent exponent. Middle: $\log\left[P_n(\Delta\rho)/f_n\right]$ vs $\log\left[g_\infty/g(E)\right]$ for various n for $L=14$ for the non-integrable (b) and the integrable (e) Ising model, and straight line fits to the ergodic data. The fits are good for $n \geq 3$. A similar fitting procedure for other system sizes yields the panels on the right, where we show that the slopes (c) and the intercepts (f) of the straight lines are simple functions of n/L.

form as (18) for P_n. We hypothesize that the scaling behavior in Eq. (18) is a generic property of non-integrable systems, and hope that this conjecture can be tested in other systems.

B. n-distinguishability of neighboring eigenstates

How do we reconcile the decrease of $P_n(\Delta\rho)/f_n$ with n in Fig. 3 with the anticipation from the ETH that expectation values of large operators, in some sense, deviate more than those of small operators? In order to resolve this counterintuitive behavior, we compute the n-distinguishability $\theta_n(\rho_1, \rho_2)$ for the same pair of neighboring eigenstates ρ_1 and ρ_2 and present the result in Fig. 5. As we discussed earlier, θ_n is the angle between two vectors $\vec{\psi}_n(\rho_1)$ and $\vec{\psi}_n(\rho_2)$, and the vectors are lists of average values of all size-n operators in the two states ρ_1, ρ_2 respectively.

As is shown in Fig. 5, θ_n increases monotonically with n for most pairs of states in the ergodic system and quickly saturates at the maximal value $\pi/2$ before n reaches $L/2$. By combining this observation with the behavior of P_n/f_n observed earlier, one can understand better what happens with increasing n. $P_n(\rho_1-\rho_2)/f_n = |\vec{\psi}_n(\rho_1)/\sqrt{f_n} - \vec{\psi}_n(\rho_2)/\sqrt{f_n}|^2$ is the square of the Eu-

clidean distance between the two vectors. Although this distance decreases with increasing n, the decrease is mainly due to the shrinking of the norm of each vector, and the angle between them actually increases. For large n the two vectors are both very short (which means a typical size-n operator has a small average value), but they are almost always exactly perpendicular. The angle is small at small n, meaning the simple-operator average values in the two neighboring eigenstates are well-correlated. In other words, as n increases, although a randomly chosen size-n operator does a worse job in distinguishing the two states in the ergodic model, there exists a particular operator – possibly a few select operators – which can distinguish the two states better. When the two vectors become perpendicular at large n, the two states can be distinguished completely if we simply use the n-size operator $\sum_\ell O_\ell^{(n)} \psi_{n\ell}(\Delta\rho)$, i.e., the projection of $\Delta\rho$ to the n-size subspace.

The behavior is markedly different for integrable systems. Here, we see that θ_n is close to $\pi/2$ already for small n, and we do not see any significant changes as n increases. This means that there exist one or a few simple operators that are excellent distinguishers of neighboring eigenstates in integrable systems, and the results of measurements in these states will not be correlated.

At the maximum of the density of states, at $E/L=0$, we see a peak of θ_n for small n. The ETH is expected to
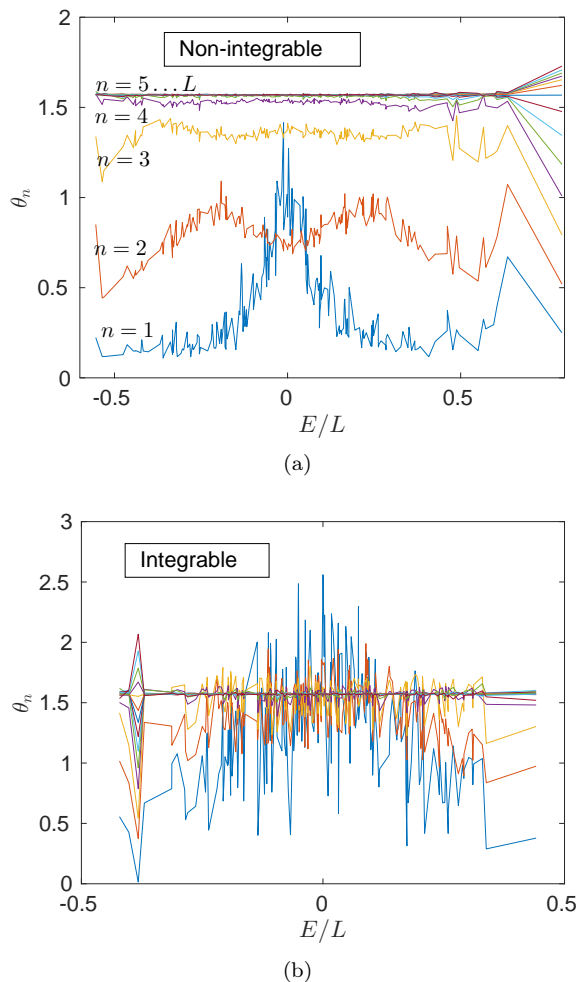
(a)

(b)

Figure 5. The angle between the projections of two neighboring eigenstates onto the space of operators of size n, θ_n as a function of energy density for various n for $L = 14$ for the non-integrable (a) and the integrable (b) Ising model. For small n, θ_n is small for most states in the ergodic model, but is large in the integrable one. For large n, it is very close to $\pi/2$ in both figures, thus proving that neighboring eigenstates are nearly orthogonal when projected onto the space of n-site operators with large n. Large θ_n at small n and large $g(E)$ ($g(E)$ is large near the middle of the spectrum and small near the edges; see Fig. 4) is due to the vectors $\rho_1^{(n)}$ and $\rho_2^{(n)}$ becoming very small in magnitude; then the angle between them is meaningless. The sharp change in θ_n at the lowest and the highest energies in the ergodic case originates from the fact that these states do not satisfy the ETH at the current system size.

work best in this regime, but the behavior of θ_n indicates that it is violated dramatically. However, this feature can be safely ignored because at infinite temperature, the simple operators' average values are almost vanishing so the angle between them is inconsequential.

V.   CONCLUSION AND DISCUSSIONS

In summary, we proposed two related new measures of thermalization, which help uncover a finer structure of the phenomenon of eigenstate thermalization than was previously known. By mapping the Heisenberg evolution of operators in a quantum many-body system onto the Schrodinger evolution of a single particle on a high dimensional graph, the complexity or size of an operator can be measured by its probability distribution in the space of all operators.

We defined the n-weight of an operator, which measures its weight in size-n operators. We studied the behavior of the n-weight for the difference between the density operators of two neighboring eigenstates in the energy spectrum, denoted as $P_n(\Delta\rho)$, which tells us how different these two states are if we only measure size-n operators. We found that $P_n(\Delta\rho)$ in the non-integrable Ising model follows a simple scaling behavior as a function of the size n and the density of states. In contrast to naive expectation, we saw that large operators on average did a *worse* job at differentiating between two neighboring eigenstates in a non-integrable system. In particular, there is a critical operator size, which is $3/4$ of the system size for spin-$1/2$ models, at which operators on average cannot distinguish between any states because they themselves are "random operators". One could always discard this conclusion in favor of intuition by saying that $P_n(\Delta\rho)/f_n$ is a misleading measure of the ETH. However, we argue against it since it is unbiased, basis-independent and physically motivated, in that directly pertains to an intuitive notion of the complexity of observables in terms of their real space spread. Thus, it helps refine our understanding of the behavior of quantum ergodic systems, as opposed to being misleading because of its counterintuitive features. In particular, we now understand more precisely, compared to our previous understanding based on the postulates of the ETH, the sense in which nearby eigenstates are distinguishable: upon increase of the operator size n, the ability of random operators to distinguish between different nearby eigenstates gets worse, but that of optimized operators gets better.

This counterintuitive conclusion was explained when we investigated the other measure of thermalization, the n-distinguishability, defined as an angle between two Hilbert space vectors, each corresponding to the projection of an operator onto the subspace of size-n operators. We saw that the angle was small for low n and saturated to $\pi/2$ for large n, which suggests that two operators (which are orthogonal in the whole space) are indeed almost orthogonal in the subspace of size-n with large n, while they are almost parallel for small n. In other words, this means that although a generic size-n operator does a poor job distinguishing two nearby eigenstates for large n, there exists a particular choice of size-n operators which can distinguish them almost perfectly. For small size operators, a random operator has an average

value that's more different in these two states than a random large size operator, simply because the expectation values increase with decreasing n. However no small operator can completely distinguish the two density operators since the two corresponding vectors are almost parallel. In short, random operators are better distinguishers for smaller n, but the best distinguishers are large operators.

The "particle-on-the-graph" picture also allows us to understand, heuristically, why the ETH holds in the first place. It follows from the fact that for vectors living in a high-dimensional space (which in this case are the states of the particle in its Hilbert space), measuring just a few components of two vectors is insufficient to deduce whether they are orthogonal or not, especially if the components along some of the measured directions are almost equal. The role of the Hamiltonian is twofold: (i) being ergodic, it ensures that the entire space of operators is connected, as opposed to integrable systems where it effectively decouples into subspaces with fixed values of the conserved quantities (ii) being a sum of simple operators, it approximately restricts the expectation values other simple operators can take in nearby eigenstates, i.e., eigenstates with the same energy density in the thermodynamic limit.

The intuition about the role of Hamiltonian can be further clarified as follows. A density operator $\rho = |\phi\rangle\langle\phi|$ of an eigenstate can be determined by the following equations:

$$[\rho, H] = 0$$
$$\text{Tr}(\rho H^m) = E^m, \ m = 1\ldots D^L - 1 \tag{19}$$

All density operators for eigenstates can be written as a linear superposition of the identity operator and H, $H^2\ldots H^{D^L-1}$. If one has access to all the coefficients of this expansion, then one can tell that two different eigenstates are mutually orthogonal. However, the coefficients of the low powers of H are slowly varying functions of E, so are almost identical for eigenstates with nearby energies. Therefore, if we restrict the measurements to operators captured by small powers of H, then it is clear why nearby eigenstates appear almost identical. The more nontrivial statement that requires non-integrability of the Hamiltonian is the fact that the expectation values of other simple operators also depend on the energy of an eigenstate smoothly, probably because the high powers of H have a negligible contribution to simple operator average values. More rigorous analytic and numerical work is required to make this discussion more complete, which we will leave for the future. We note that phase space based reasons for why isolated quantum systems fulfil the basic tenets of statistical mechanics have been suggested in the past to argue that most systems, at most times and for most observables, behave as if they belonged to a thermal ensemble [29–31]. The proofs there were based on Levy's lemma which is the analog of the law of large numbers for vectors in a high-dimensional space.

All the results in this work concern expectation values of operators in eigenstates. The off-diagonal matrix elements of an operator between different eigenstates $\langle n|O|m\rangle$ are responsible for time-evolution properties of the system. Whether thermalization occurs in time evolution of a state that is not an eigenstate, and how fast it occurs, depends on two properties, the off-diagonal matrix elements of observables, and the energy difference between eigenstates. As long as the energy differences are sufficiently incommensurate, time evolution causes decoherence and thus leads to equilibration [29–34]. However, different operators may thermalize at different rates, which is an interesting problem that can be studied using the new measures we defined.

[1] M. V. Berry, Journal of Physics A: Mathematical and General **10**, 2083 (1977), URL http://stacks.iop.org/0305-4470/10/i=12/a=016. I

[2] J. M. Deutsch, Phys. Rev. A **43**, 2046 (1991), URL http://link.aps.org/doi/10.1103/PhysRevA.43.2046. I

[3] M. Srednicki, Phys. Rev. E **50**, 888 (1994), URL http://link.aps.org/doi/10.1103/PhysRevE.50.888. I

[4] J. R. Garrison and T. Grover, ArXiv e-prints (2015), 1503.00729. I, IV

[5] M. Rigol, V. Dunjko, and M. Olshanii, Nature **452**, 854 (2008), ISSN 1476-4687, URL http://dx.doi.org/10.1038/nature06838. I

[6] M. Rigol, Phys. Rev. A **80**, 053607 (2009), URL http://link.aps.org/doi/10.1103/PhysRevA.80.053607. IV

[7] M. Rigol and M. Srednicki, Physical Review Letters **108**, 110601 (2012), ISSN 0031-9007, URL http://link.aps.org/doi/10.1103/PhysRevLett.108.110601.

[8] M. Rigol, Phys. Rev. Lett. **112**, 170601 (2014), URL http://link.aps.org/doi/10.1103/PhysRevLett.112.170601.

[9] S. Khlebnikov and M. Kruczenski, Physical Review E **90**, 050101 (2014), ISSN 1539-3755, URL http://link.aps.org/doi/10.1103/PhysRevE.90.050101.

[10] S. Sorg, L. Vidmar, L. Pollet, and F. Heidrich-Meisner, Phys. Rev. A **90**, 033606 (2014), URL http://link.aps.org/doi/10.1103/PhysRevA.90.033606.

[11] M. Marcuzzi, J. Marino, A. Gambassi, and A. Silva, Phys. Rev. Lett. **111**, 197203 (2013), URL http://link.aps.org/doi/10.1103/PhysRevLett.111.197203. I

[12] H. Kim, T. N. Ikeda, and D. A. Huse, Phys. Rev. E **90**, 052105 (2014), URL http://link.aps.org/doi/10.

1103/PhysRevE.90.052105. I, IV

[13] V. Khemani, A. Chandran, H. Kim, and S. L. Sondhi, Phys. Rev. E **90**, 052133 (2014), URL http://link.aps.org/doi/10.1103/PhysRevE.90.052133.

[14] V. Alba, Phys. Rev. B **91**, 155123 (2015), URL http://link.aps.org/doi/10.1103/PhysRevB.91.155123.

[15] W. Beugeling, R. Moessner, and M. Haque, Phys. Rev. E **91**, 012144 (2015), URL http://link.aps.org/doi/10.1103/PhysRevE.91.012144.

[16] W. Beugeling, R. Moessner, and M. Haque, Phys. Rev. E **89**, 042112 (2014), URL http://link.aps.org/doi/10.1103/PhysRevE.89.042112.

[17] T. N. Ikeda, Y. Watanabe, and M. Ueda, Phys. Rev. E **84**, 021130 (2011), URL http://link.aps.org/doi/10.1103/PhysRevE.84.021130.

[18] P. Reimann, New Journal of Physics **17**, 055025 (2015), URL http://stacks.iop.org/1367-2630/17/i=5/a=055025. I

[19] E. Lubkin, Journal of Mathematical Physics **19**, 1028 (1978), ISSN 00222488, URL http://scitation.aip.org/content/aip/journal/jmp/19/5/10.1063/1.523763. I

[20] D. N. Page, Phys. Rev. Lett. **71**, 1291 (1993), URL http://link.aps.org/doi/10.1103/PhysRevLett.71.1291.

[21] S. K. Foong and S. Kanno, Phys. Rev. Lett. **72**, 1148 (1994), URL http://link.aps.org/doi/10.1103/PhysRevLett.72.1148.

[22] J. Sánchez-Ruiz, Phys. Rev. E **52**, 5653 (1995), URL http://link.aps.org/doi/10.1103/PhysRevE.52.5653.

[23] S. Sen, Phys. Rev. Lett. **77**, 1 (1996), URL http://link.aps.org/doi/10.1103/PhysRevLett.77.1. I

[24] M. B. Hastings, I. González, A. B. Kallin, and R. G. Melko, Phys. Rev. Lett. **104**, 157201 (2010), URL http://link.aps.org/doi/10.1103/PhysRevLett.104.157201. II

[25] B. L. Altshuler, Y. Gefen, A. Kamenev, and L. S. Levitov, Phys. Rev. Lett. **78**, 2803 (1997), URL http://link.aps.org/doi/10.1103/PhysRevLett.78.2803. II

[26] C. Neuenhahn and F. Marquardt, Phys. Rev. E **85**, 060101 (2012), URL http://link.aps.org/doi/10.1103/PhysRevE.85.060101. II

[27] V. Ros, M. Mueller, and A. Scardicchio, Nuclear Physics B **891**, 420 (2015), ISSN 0550-3213, URL http://www.sciencedirect.com/science/article/pii/S0550321314003836. II

[28] M. Rigol, Phys. Rev. Lett. **103**, 100403 (2009), URL http://link.aps.org/doi/10.1103/PhysRevLett.103.100403. IV

[29] S. Popescu, A. J. Short, and A. Winter, eprint arXiv:quant-ph/0511225 (2005), quant-ph/0511225. V

[30] S. Popescu, A. J. Short, and A. Winter, Nat Phys **2**, 754 (2006), ISSN 1745-2473, URL http://dx.doi.org/10.1038/nphys444.

[31] N. Linden, S. Popescu, A. J. Short, and A. Winter, Phys. Rev. E **79**, 061103 (2009), URL http://link.aps.org/doi/10.1103/PhysRevE.79.061103. V

[32] V. Yukalov, Laser Physics Letters **8**, 485 (2011), ISSN 1612-202X, URL http://dx.doi.org/10.1002/lapl.201110002.

[33] V. Yukalov, Physics Letters A **376**, 550 (2012), ISSN 0375-9601, URL http://www.sciencedirect.com/science/article/pii/S0375960111013685.

[34] V. Yukalov, Physics Letters A **375**, 2797 (2011), ISSN 0375-9601, URL http://www.sciencedirect.com/science/article/pii/S0375960111007353. V